



Removal of Methylene Blue from Aqueous Solutions by Anatase doped on Kaolin and Zeolite

Amany W. Ali*, E. M. Ezzo, S. A. Hassan and N. G. Mosa

Ain Shams University, Asmaa Fahmi St, Al Golf, Heliopolis, Cairo, Egypt



CrossMark

Abstract

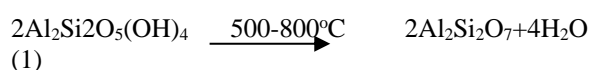
The nanoparticles of Ti/Z I, Ti/Z II, Ti/Ka I and Ti/Ka II solids were prepared by impregnation with calculated 10 and 15 mmole of solid titanium oxide over zeolite and kaolin as supported materials. These were examined using TGA&DTA, XRD, EDX, SEM, TEM, and BET, respectively to determine their physicochemical characteristics. TEM and SEM results showed that the particle sizes of the prepared and investigated solids lie in the ranged (11-100) nm. The Kinetic removal of Methylene blue dye (MB) was studied by the four prepared solids by different Kinetic conditions as (effect of weight of adsorbents, concentration of MB dye, contact time and pH) in aqueous synthetic solution of MB. It was found that the Ti/Ka II had maximum removal 99.9% at concentration of dye 10 ppm, weight of adsorbents 0.01g, contact time 120 min and pH = 3.

Keywords: Removal of methylene blue dye by TiO₂/zeolite and TiO₂/metakaolin.

1. Introduction

Many significant issues arise when water is contaminated with such dyes, including an increase in the toxicity and chemical oxygen demand of the effluent, which is harmful to photochemical processes. These dyes are all synthetic and made up of complicated aromatic compounds. When released into water streams, the majority of them appeared inert and non-biodegradable while being capable of causing cancer and mutations [1-3]. Due to their great capacity for the adsorption of organic compounds, activated carbon is the most popular adsorbent and has been shown to be effective in the removal of colored organic species. TiO₂/zeolite and TiO₂/metakaolin are being investigated as replacements to inexpensive, less effective adsorbents due to their lower cost and easier regeneration, respectively as concluded [4, 5].

Zeolites are crystalline aluminosilicates made of AlO₄ and SiO₄ tetrahedra that are joined to one another by their oxygens to form regular interconnecting pores and tunnel [6-11]. At 500°C, thermal activation of kaolin was performed first. Raw kaolin undergoes thermal processing to produce metakaolin via an endothermic de-hydroxylation reaction as reported [12](Eq. 1).



Kaolin 500-850°C metakaolin

Consequently, alkali metal hydroxides as aqueous solutions were used to treat the metakaolin at a comfortable temperature. The reaction mixture's composition affects the type of zeolite that forms. Zeolite and kaolin criteria have been utilized, and their effects on the kinds and physicochemical properties of the solids they produced have been investigated.

Using the Langmuir adsorption isotherm model, the adsorption behavior of the produced nanoparticles was examined for the removal of methylene blue. Several industries produce effluents that contain dyes in the course of their operations. Particularly water-intensive industries like textiles release significant amounts of dyes into their effluents. One type of pozzolanic substance is metakaolin(MK). High-grade of kaolinite was calcined at temperatures between 600°C and 900°C, respectively to produce high reactive calcined clay, with another name [13-19].

The most popular adsorbent for industrial applications and various studies of the breakdown of different azo dyes in textile effluent is titanium dioxide. Anatase and rutile are the two most widespread crystalline forms of TiO₂, and rutile's crystalline size is always greater than anatase's. For most purposes, the third structural type, known as brookite, is an orthorhombic structure that is rarely

*Corresponding author e-mail: amanywaheed8@gmail.com.; (Amany W. Ali)

Receive Date: 14 February 2023, **Revise Date:** 05 March 2023, **Accept Date:** 07 March 2023

First Publish Date: 07 March 2023

DOI: 10.21608/EJCHEM.2023.193903.7609

©2023 National Information and Documentation Center (NIDOC)

utilized and not especially attractive[20-23].

The chemical compound methylene blue has the IUPAC name 3,7-bis(Dimethylamino)-phenothiazin-5-ium chloride and the molecular formula $C_{16}H_{18}ClN_3S$, as shown in Figure (1).

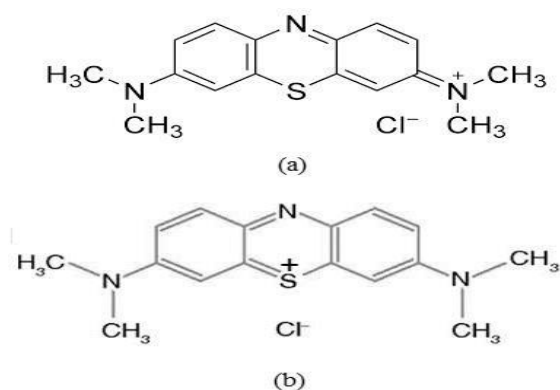


Fig.1. Molecular structure scheme of the methylene blue

The objective of this work is to determine if two adsorbents, TiO_2 /zeolite and TiO_2 /metakaolin, produced by impregnation, are suitable for the adsorption of MB dye from aqueous solution at various ml mole concentrations of TiO_2 .

2. Materials and Methods of preparation

2.1. Materials

Methylene blue is a cationic dye provided from Riedel deHaen, zeolite provided from Sigma – Aldrich, Metakaolin provided from Hems Construction Chemical Company, Titanium dioxide TiO_2 provided from RANKEM Laboratory chemical reagents, HCl 98% provided from Bio Chem Laboratories, $AgNO_3$ provided from Bio Chem Laboratories, Ethanol CH_3CH_2OH provided from Bio Chem Laboratories, NaOH provided from Bio Chem Laboratories and Sulphuric acid H_2SO_4 98% provided from Bio Chem Laboratories.

2.2. Methods of preparation of adsorbents

There Adsorbents were made using the impregnation technique. The zeolite was grinded into a powder, cleaned with distilled water, and dried for two hours in an oven set at $110^\circ C$. A 40 g of the precipitate was activated by being soaked in 60 ml of HCl 0.4 M. After 4 hours of shaking at 100 rpm, the

mixture was filtered out. The precipitate was rinsed in distilled water until the chloride ions were removed (the filtrate was tested with $AgNO_3$ 1M). The precipitate was then dried for two hours at $110^\circ C$.

For preparation the solid TiO_2 /zeolite, 15 g of activated zeolite was wetted with the least amount of water to form a semi liquid paste then mixed with 12.2 g and 18.2g of TiO_2 and ethanol was added in range 70-75 ml to produce (10 and 15 mmol TiO_2 / g zeolite). The mixture was stirred for 3 hours at room temperature then dried at $120^\circ C$ for 5 hours[24].

Treated metakaolin was prepared by diluting 100.00 g of metakaolin in 1250 ml of 2M H_2SO_4 . The mixture was stirred with a magnetic stirrer for 4 hours at $80^\circ C$. At the end, the mixture was filtered off and then dried overnight at $80^\circ C$. The dried solid was mixed with 134.04 g of NaOH. The mixture was grinded to obtain a homogenous fusion of solid. The solid then calcined at $550^\circ C$ for 20 minutes. The calcined material was then mixed with 633.8 ml of distilled water, stirred at room temperature for 24 hour, reflux at $100^\circ C$ for 3 hours and filtered with washing with distilled water and oven-dried at $80^\circ C$ overnight[25].

For preparation the solid TiO_2 /treated metakaolin, 20 g of treated metakaolin was wetted with the least amount of water to form a semi liquid paste then mixed with 16.29 g and 24.28 g of TiO_2 and ethanol was added in range 80 ml to produce (10 and 15 mmol TiO_2 / g treated metakaolin). The mixture was stirred for 3 hours at room temperature then dried at $120^\circ C$ for 5 hours [25].

3. The Physicochemical Studies of the Adsorbent

3.1 XRD measurements

The Bruker D8 DISCOVER Diffractometer was used to do the X-ray diffraction observations using Cu-K radiation ($\lambda = 1.54060$ Angstrom). The relative intensity data were obtained throughout a 2θ range of $5^\circ - 100^\circ$, the chart was used to determine the 2θ values and relative intensities (I/I₀), and JCPDS cards were used to identify the minerals in the core materials. All samples were degassed for 4 hours at $500^\circ C$ before taking the measurements.

Table.1. Composition of The catalysts used (calcined at temperature of $500^\circ C$ for 4h.

Adsorbent	Adsorbent symbols.,	Experimental EDX (At%)			
		Na	Al	Si	Ti
TiO_2 /zeolite (10 mmol)	Ti/Z I	18.56	23.20	23.33	34.91
TiO_2 /zeolite (15 mmol)	Ti/Z II	16.98	17.86	15.96	49.21
TiO_2 /kaolin (10 mmol)	Ti/Ka I	20.73	22.90	25.25	31.13
TiO_2 /kaolin (15 mmol)	Ti/KaII	19.79	21.15	22.92	36.14

3.2 Textural characteristics (BET)

The nitrogen adsorption isotherms were measured using a Quantachrome NOVA touch 2LX at -196°C (77k), and the results were used to calculate the surface properties of the different zeolites, including surface area (BET), total pore volume (V_p), and average pore radius (r'). Before taking the measurements, all samples were degassed at 500 oC for 4 hours at a lowered pressure of 1.3 mPa. The anatase content over zeolite and kaolin were determined for the prepared solids Ti/Z I, Ti/Z II, Ti/Ka I, and Ti/Ka II by EDX for Na, Al, Si and Ti, given in table (1).

3.3 Thermogravimetric analysis (TGA)

Thermogravimetric analysis was performed on all fresh solid samples using a thermobalance and a Shimadzu-TGA in the temperature range of 0 to 900°C. In an environment of air, the samples were heated at a rate of 10°C min⁻¹.

3.4 Differential thermal analysis (DTA)

Shimadzu-TGA (Germany) was used to determine differential thermal analysis for fresh pieces of all solid samples in the temperature range of 0 to 900°C using a thermobalance. The samples heated at a rate of 10°C min⁻¹ in an environment of air.

3.5 Transmission electron microscopy (TEM)

AJEOL JEM 2100 measuring devices running at 200kV were used for TEM research. An ultrahigh resolution polar piece (point resolution: 1.9Å) is included with the microscope. A holey carbon film supported by a Cu grid (100-150 mesh) was used to drop and dry the colloidal solution to create the specimen for TEM examination.

3.6 Scanning electron microscopy (SEM)

For all prepared solid samples, SEM studies were measured using INSPECT-SEI running at 200KV.

4. Removal Experiments

Studying the impact of dye removal by Ti/Z I, Ti/Z II, Ti/Ka I and Ti/Ka II solids. The solutions for the adsorption studies were diluted to the required concentrations from a stock solution of 1000 mg/l MB. The batch approach was used to adsorb MB on TiO₂/zeolite and TiO₂/metakaolin at room temperature (25±0.1°C) in a 250-ml conical flask. Role of concentration of dye, weight of adsorbent, pH and time of contact were discussed. By adjusting the pH of the adsorptive solution using (0.1 N) HCl and (0.1 N) NaOH solutions, the effect of pH was investigated, results of the experiment showed that the pH of dye without adding any standard solution (6.7). The absorbance of dye was studied by UV-Vis spectrometer.

The amount of dye adsorbed per mass unit of adsorbent at time t, Q_e (mg/g) and dye removal %, were calculated by the following equations

$$\% Re = 100 \left(\frac{C_i - C_f}{C_i} \right) \quad (2)$$

$$Q_e = \frac{(C_i - C_f)V}{w} \quad (3)$$

where C_i is the initial concentration of MB and C_f is the final concentration of MB after the sorption by adsorbents, V is the volume of solution (in L) and W is the mass of adsorbent (in g).

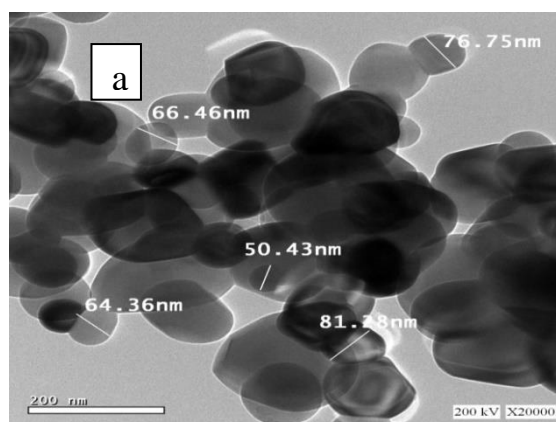
5. Results and Discussion

5.1. Transmission and scanning electron microscopy (TEM), (SEM)

For all produced solid samples, TEM studies were performed using a JEOL JEM 2100 working at 200kV at a magnification of 1:1500000 x, while SEM studies were measured using an INSPECT-SEI operating at 200kV. Figure (2) displays the TEM images and SEM images of Ti/Z I and Ti/Ka I. It is evident that 4A zeolite and kaolin have dispersed TiO₂ particles coated on their surfaces. All produced solids, as seen by TEM micrographs, have particle sizes between 11 and 100 nm, demonstrating that solid materials exist on the nanometer scale.

5.2. Thermal gravimetric analysis TGA & DTA

According to Figure(3) of the TGA curves for Ti/Z II and Ti/K II, weight loss occurs in four phases, with the first two stages being the elimination of physisorbed water and the third step possibly being the creation of oxide. With a total weight loss of 4.93 and 6.68% for Ti/Z II and Ti/K II, respectively, the four samples stay unchanged up to 800°C. The energy of activation of each step was calculated and is given in figure (3a, 3b). The DTA curves for Ti/Z II and Ti/K II is shown in figure (3c, 3d). Figure (3c) displays one endothermic peak at 126.51°C. The DTA curve for Ti/Ka II catalyst is shown in figure (3d).



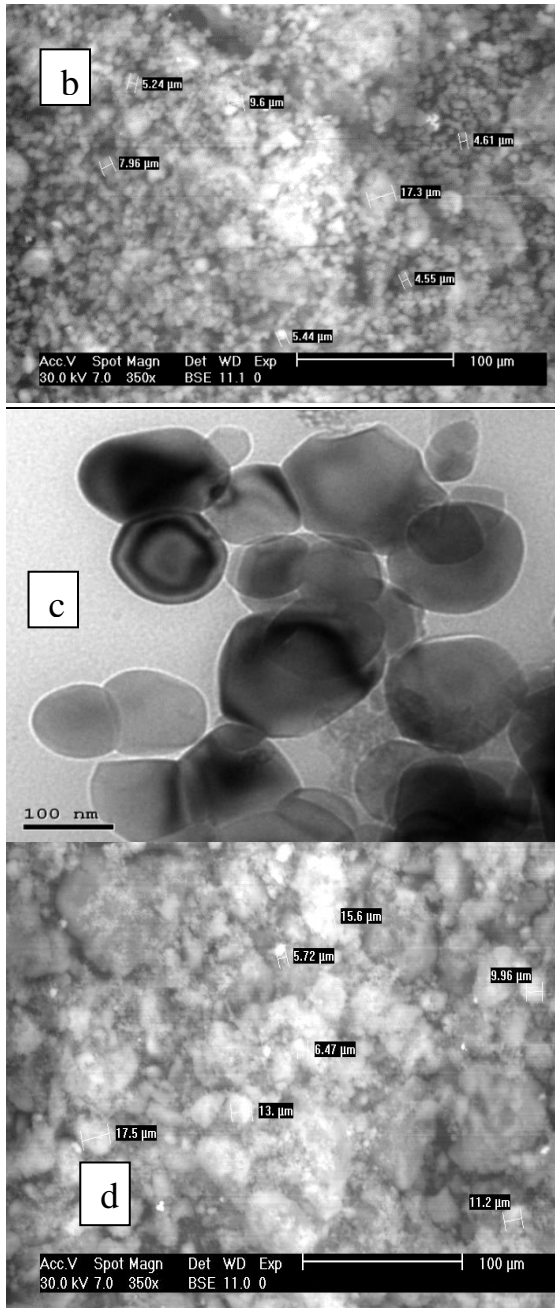


Fig.2. TEM and SEM photos of (a),(b) Ti/Z I; (c),(d) Ti/K I

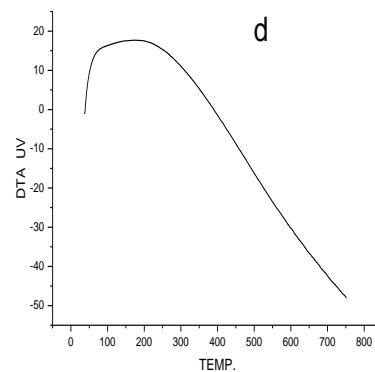
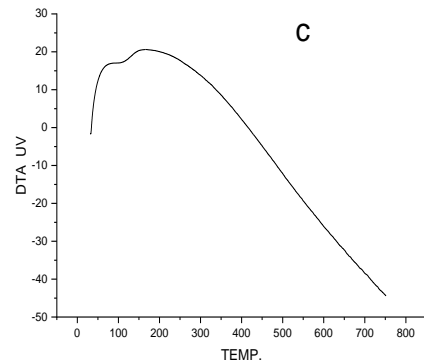
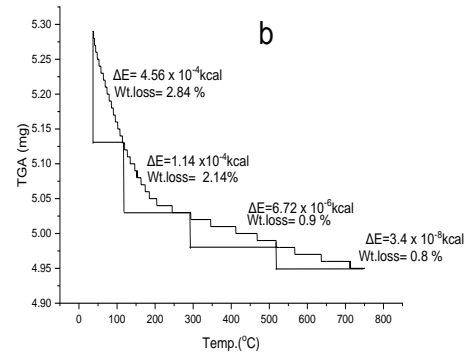
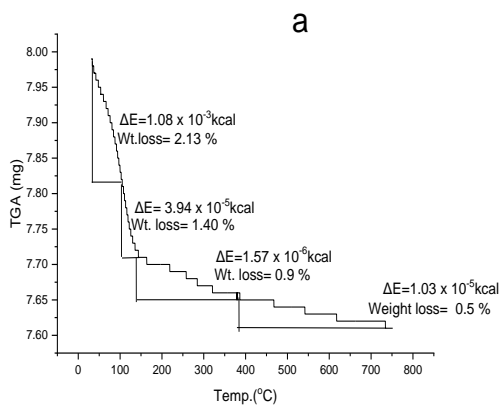


Fig.3. Differential Thermal Analysis (DTA) of, (a) Ti/Z I, (b) Ti/Ka II, (c) Ti/Z II and (d) Ti/Ka II



5.3. XRD measurements

At 500°C for four hours, the thermal products of Ti/ZI and Ti/KaI and their X-ray diffraction patterns (XRD) were obtained. In figure (4) the diffracted patterns are shown. The peak intensities' variations against to 2θ are shown in the figure. Poor crystallinity may be seen in the results of the Ti/ZI and Ti/KaI calcinations at 500°C. In general, rising the calcination temperature to 900°C helped to increase the crystallinity. After being loaded with titanium oxide, both synthetic and zeolite made from Egyptian metakaolin showed structural changes and suffered amorphization. Based on the information provided and shown in figure (4), it is evident that

synthetic zeolite has a cubic lattice and the chemical formula $\text{Na}_{12} \text{Al}_{12} \text{Si}_{12} \text{O}_{48} \cdot 27\text{H}_2\text{O}$. The zeolite feature diffraction peaks are at $2\theta = 7.13^\circ, 10.13^\circ, 12.42^\circ, 16.07^\circ, 20.39^\circ, 22.86^\circ, 23.97^\circ, 29.94^\circ, 30.83^\circ, 35.76^\circ, 44.18^\circ, 52.62^\circ, 54.29^\circ, 69.14^\circ, 71.04^\circ$ and 78.08° . TiO_2 present with tetragonal lattice structure and diffraction peaks at $2\theta = 25.30^\circ, 38.57^\circ, 48.07^\circ, 53.88^\circ, 55.07^\circ, 62.69^\circ, 70.30^\circ$ and 76.04° . Stronger TiO_2 peak at $2\theta = 25.30^\circ$ may mean that the anatase phase of TiO_2 is still present. The zeolite that was prepared from Egyptian metakaolin has chemical formula $\text{Al}_2 \text{H}_4 \text{O}_9 \text{Si}_2$ with Triclinic lattice structure and diffraction peaks at $2\theta = 12.36^\circ, 19.84^\circ, 24.87^\circ, 31.53^\circ, 35.12^\circ, 41.28^\circ, 55.29^\circ, 59.82^\circ$ and 78.00° .

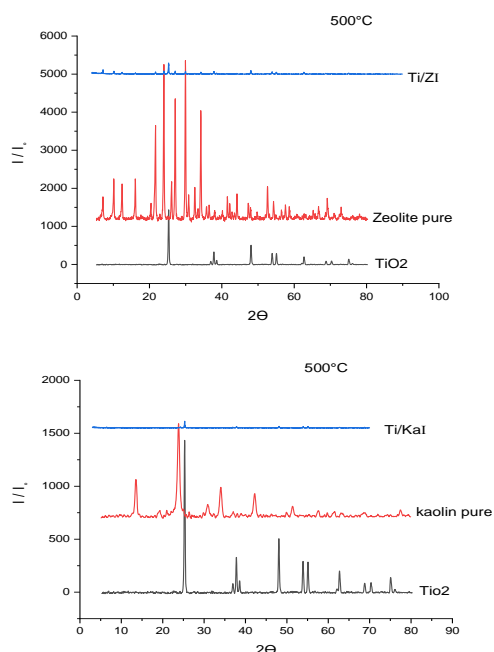


Fig.4. The X-ray diffractograms of prepared solids (Zeolite, Kaolin, TiO_2 , Ti/Z I and Ti/Ka I).

5.4. Textural characteristics (BET)

Figure (5a, b) shows visually the nitrogen gas adsorption-desorption isotherms on Ti/ZII and Ti/KaII after calcining at 500°C for 4 hours at liquid nitrogen temperature of -195°C . The isotherms could be categorized as macroporous or nonporous type III isotherms. Table.1 displays the textural characteristics determined from N_2 adsorption/desorption studies.

Table (2): Textural characteristics of the prepared adsorbents (calcined at a temperature of 500°C for 4h).

Adsorbent	$S_{\text{BET}}, \text{m}^2.\text{g}^{-1}$	Pore volume, $\text{cc}.\text{g}^{-1}$	Average pore radius, nm
Ti/Z II	634.54	0.10	1.48
Ti/Ka II	547.45	0.08	1.71

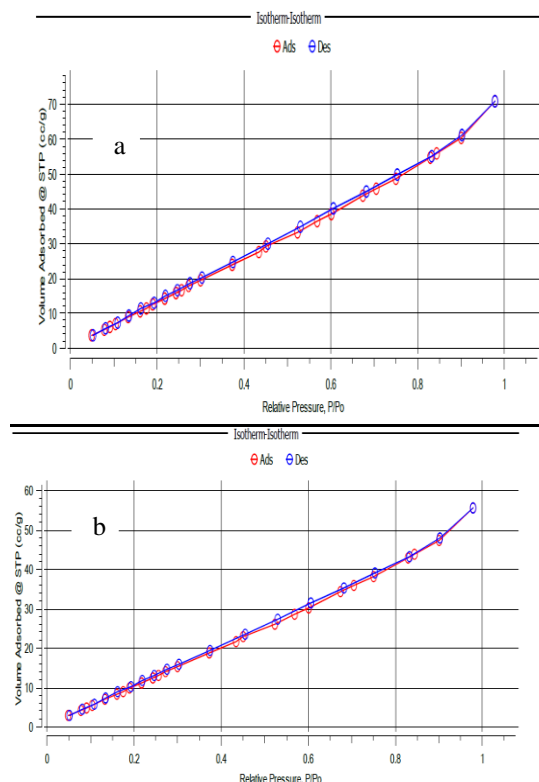


Fig .5.The nitrogen adsorption/desorption isotherm of (a) Ti/ZII and (b) Ti/KaII

6. Removal of Methylene Blue Dye

The removal percentage of the prepared Ti/Z I (adsorbent 1), Ti/Z II (adsorbent 2), Ti/Ka III (adsorbent 3) and Ti/Ka IV (adsorbent 4) solids toward the treatment of an aqueous solution of the dye methylene blue is measured in this study. Initial dye concentration, contact time, adsorbent dosage, and pH are among the variables examined. Freundlich and Langmuir isotherm models were applied to the equilibrium data.

6.1. Effect of MB concentration and weight of adsorbents

By adjusting the MB concentrations (7, 10, 15 and 20 ppm) and using 0.01 g of adsorbents for 3 hours at a constant room temperature ($25 \pm 0.1^\circ\text{C}$) and constant pH (7.0 ± 0.2), the % removal of MB was thus determined. Figure (6) illustrates how initial dye concentration affects the rate at which MB is removed from Ti/Z I and Ti/Z II. At concentration (7 ppm), the removal percent of Ti/Z II initially exceeds that of Ti/Z I, but at concentration (10 ppm, the reverse occurred). The removal percentage of Ti/Z I reduced with an increase in dye concentration, whereas the removal percentage of Ti/Z II stayed unchanged.

It can be concluded from calculating the specific removal (mean overall removal percent/ $S_{\text{BET}} \text{m}^2.\text{g}^{-1}$) of Ti/Z I ($131.10 \text{ \%}.\text{g}/\text{m}^2$) and Ti/Z II ($149.04 \text{ \%}.\text{g}/\text{m}^2$) that Ti/Z II has more removal activity than Ti/Z I.

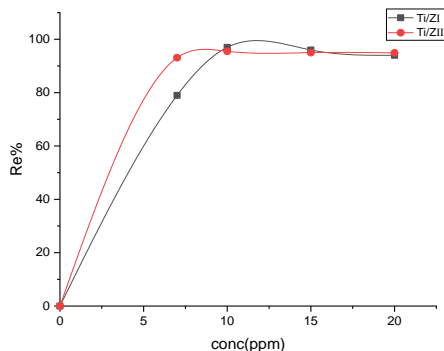


Fig.6. Effect of initial concentration on the adsorption of M.B dye by Ti/Z I and Ti/Z II

Figure (7) illustrates how initial dye concentration affects the rate at which MB is removed from Ti/ka I and Ti/ka II. Because there were no active sites present at higher dye concentrations and the adsorption sites on the adsorbent were completely adsorbed, the percentage of dye removal was initially found to be high and did not change as M.B concentration increased.

It can be concluded from calculating the specific removal (mean overall removal percent/ $S_{BET} \text{ m}^2 \cdot \text{g}^{-1}$) of Ti/KaI (162.20%.g/m²) and Ti/KaII (178.55%.g/m²) that Ti/ka II has more removal activity than Ti/ka I.

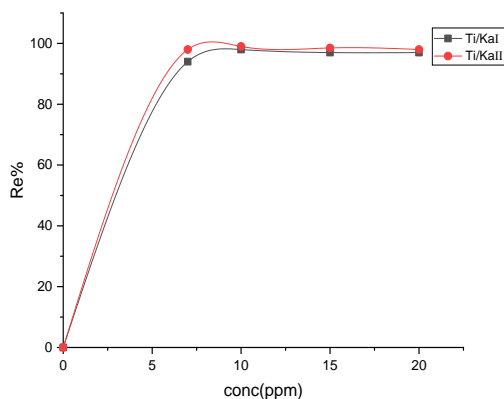


Fig.7. Effect of initial concentration on the adsorption of M.B dye by Ti/Ka I and Ti/Ka II

By adjusting the weight of adsorbents (0.01, 0.03, 0.05, and 0.07 g) with a concentration of 10 ppm for 3 hours at a constant room temperature of (25 ± 0.1°C) and a constant pH of (7.0 ± 0.2), the % removal of MB was thus studied. Figure (8) illustrates how the weight of the adsorbent affects the adsorption of MB. It can be seen that the percentage of dye removal was first determined to be high and remained unchanged as the dose increased.

It can be concluded from calculating the specific removal (mean overall removal percent/ $S_{BET} \text{ m}^2 \cdot \text{g}^{-1}$) of Ti/Z I (138.60 %.g/m²) and Ti/Z II (152.04

%.g/m²) that Ti/Z II has more removal activity than Ti/Z I.

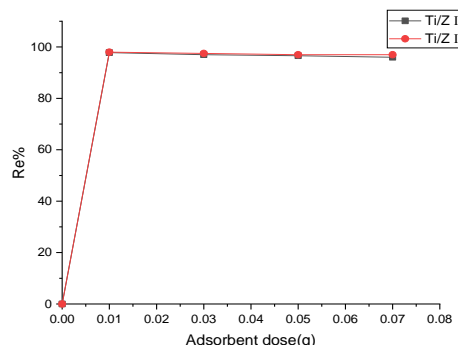


Fig.8. Effect of adsorbent dose on the adsorption of M.B dye by Ti/Z I and Ti/ZII

Figure (9) illustrates how the adsorbent weight affects the adsorption of MB on Ti/ka I and Ti/ka II. Greater surface area and the availability of more adsorption sites can be responsible for the first, sharp rise in adsorption. Then the decrease or stability is due to All active sites on the adsorbent surface were then occupied, and any increase in adsorbent dosage did not yield a higher MB uptake.

It can be concluded from calculating the specific removal (mean overall removal percent/ $S_{BET} \text{ m}^2 \cdot \text{g}^{-1}$) of Ti/KaI (161.40%.g/m²) and Ti/Ka II (179.61%.g/m²) that Ti/Ka II is more active than Ti/Ka I.

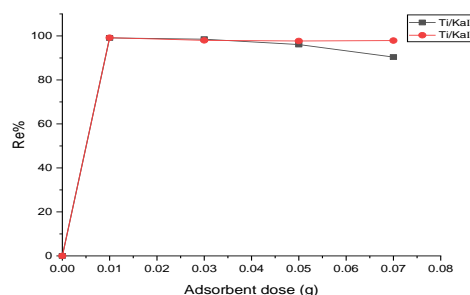


Fig.9. Effect of adsorbent dose on the adsorption of M.B dye by Ti/Ka I and Ti/Ka II

6.2. Effect of contact time

Thus, by adjusting the contact time from 5 to 180 min with 0.01 g of adsorbents, at constant concentrations of 10 ppm at constant room temperature (25 ± 0.1°C), and at constant pH (6.8 ± 0.1), the percentage removal of MB was studied. Figure (10) illustrates how contact time affects the rate at which MB is removed on Ti/Z I and Ti/Z II. It is possible to see that as the contact time with two adsorbents increased, so does the percentage of adsorption. At 120 minutes, the adsorbent Ti/Z I reached its maximum removal percentage (97%) while Ti/Z II reached its maximum removal percentage (96%). These results show that Ti/Z I is better than Ti/Z II.

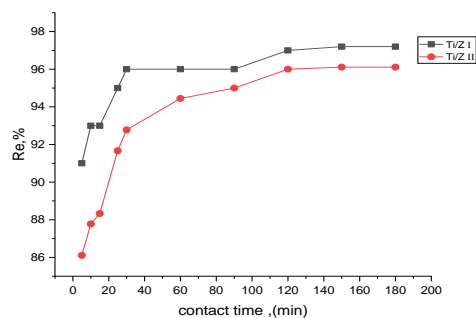


Fig.10.Effect of contact time on the adsorption of M.B dye by Ti/Z I and Ti/Z II

Figure (11) illustrates how contact time affects the rate at which MB is removed from Ti/Ka I and II. It is possible to see that as the contact time of two adsorbents increased, so does the percentage of adsorption. At 120 minutes, the adsorbent Ti/Ka I reached its maximum removal percentage (97.8%), whereas Ti/Ka II reached its maximum removal percentage (99.2%). These results show that Ti/Ka II is better than Ti/Ka I.

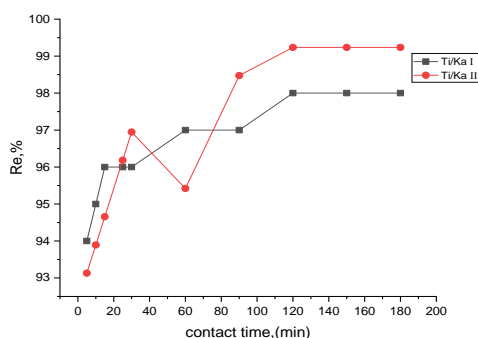


Fig.11.Effect of contact time on the adsorption of M.B dye by Ti/Ka I and Ti/Ka II

6.3. Effect of pH

An essential factor that can regulate the adsorption process is the dye solution's initial pH. At various pH levels, the removal of MB was studied as a function of pH (3, 4, 9 and 10). In the studies, 0.01 g of adsorbents was used, with a contact time of 120 min at constant room temperature ($25 \pm 0.1^\circ\text{C}$) and an initial concentration of 10 ppm. Figure (12) shows how pH affects the percentage of removal. The maximum removal percentage for Ti/Z I was 98% at pH = 4 and for Ti/Z II it was 99.6% at pH = 3. These values are therefore ideal because they are near to the $\text{pK}_a = 3.8$ of the MB. It can be concluded from these results that Ti/Z II give higher removal percent in acidic medium (pH=3) than Ti/Z I.

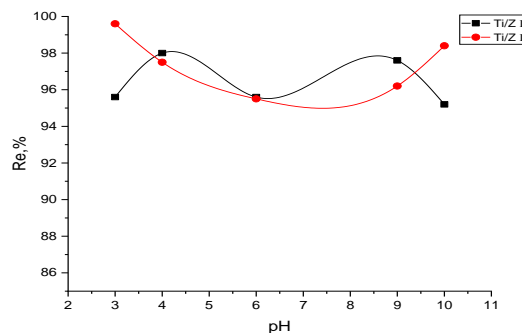


Fig.12.Effect of pH on the adsorption of M.B dye by Ti/Z I and Ti/Z II

Figure (13) shows how pH affects the percentage of removal. For Ti/Ka I and Ti/Ka II, the maximum removal percentages were 98.5% at pH = 4 and 99.9% at pH = 3, respectively. These values are therefore ideal because they are near to the $\text{pK}_a = 3.8$ of the MB. Zeolite and kaolin had pH_{PZC} values of 5.66 (acidic value) and 10.17 (basic value), respectively. Materials' surfaces are positive below the pH_{PZC} whereas they are negative at pH levels above the pH_{PZC} . Unfortunately, the pH values taken into consideration at this moment prevent a conclusive explanation for this issue from being produced. In general, the surface charge of the adsorbent, the degree of ionization of the adsorptive molecule, and the extent of functional group dissociation on the active sites of the adsorbent all appear to have an impact on the adsorptive characteristics of the adsorbent below and above the pH of maximum adsorption[26]. It can be concluded from these results that Ti/Ka II give higher removal percent in acidic medium than Ti/Ka I.

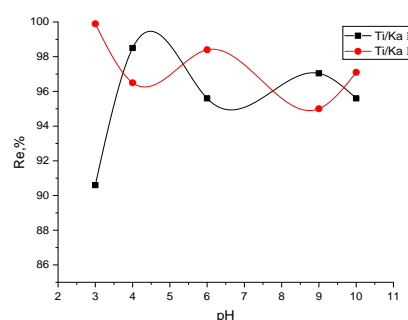


Fig.13.Effect of pH on the adsorption of M.B dye by Ti/Ka I and Ti/Ka II

7. Adsorption Isotherm

Adsorption isotherm models, which represent the surface characteristics and affinity of the adsorbent toward the adsorbate, characterize the adsorption system. The analysis of adsorption data utilized both the Freundlich and Langmuir adsorption isotherm models. While Freundlich assumes multilayer of adsorption on heterogeneous surface of the adsorbent, the Langmuir isotherm model suggests monolayer adsorption of dyes on the homogeneous surface of the adsorbent.

The Langmuir isotherm is :

$$C_e / Q_e = 1/Q_m b + C_e / Q_m \quad (4)$$

The amount of dye adsorbed is expressed by Q_e (mg/g), the equilibrium concentration is C_e (mg/L), and Q_m and b are the Langmuir constants of adsorption capacity and adsorption's energy. The Langmuir isotherms may be applicable, according to the linear plots of C_e / Q_e vs C_e . The slope and intercept of the plots have been used to determine the values of Q_m and b .

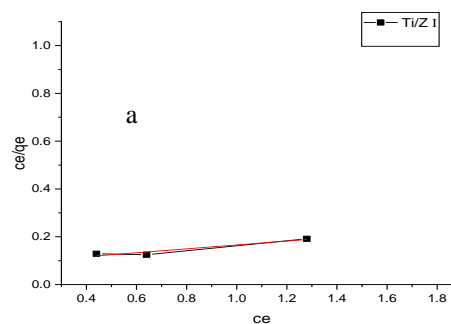
$$\ln Q_e = \ln K_f + 1/n \ln C_e \quad (5)$$

Eq. (5) worked as a representation of the Freundlich isotherm

Where K_f and n are constants including the variables affecting the adsorption capacity and intensity, respectively, and Q_e is the quantity of dye adsorbed (mg/g), C_e is the equilibrium concentration of dye in solution (mg/L), and The Freundlich isotherm is obeyed for the adsorption of dyes, as shown by linear graphs of $\ln Q_e$ vs $\ln C_e$.

To analyze the experimental data, the linear Langmuir and Freundlich isotherm figures (14), (15a,b) were utilized. The values of Q_m and b were shown in table (3) based on the slope and intercept of the plots. Given the reported correlation coefficient (R^2), we concluded that the Langmuir model is better than the Freundlich model.

According to table (3), Ti/Z II exhibits greater adsorption efficiency (Q_m) than Ti/Z I. The energy of the adsorption process is represented by the constant b in the Langmuir equation. The free energy decreases with increasing values of the constant b , making the process more suitable since less energy is needed to maintain it. The process' endothermic nature is evident from the observed b value. For the adsorption of dyes on the adsorbents, the Freundlich equation was used. Table (3) provides K_f and n value information, Adsorption intensity (n) is a measure of the bond



energies between the dye and the adsorbent. Since the values of n are higher than 1, the adsorption is advantageous. The results show that Ti/Z I adsorbs the dye more favorably than Ti/Z II because the value of n is higher than unity in that case.

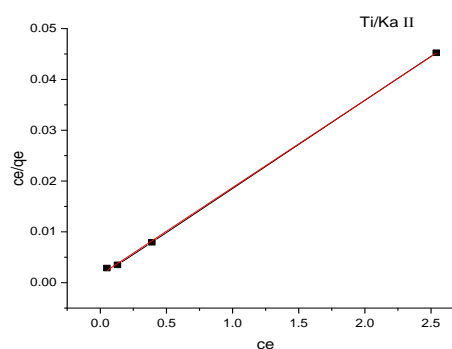


Fig.(14): linear Langmuir isotherm for the adsorption of methylene blue dye by (a)Ti/Z I, (b)Ti/Ka II

According to table (4), Ti/Ka II exhibits greater adsorption efficiency (Q_m) than Ti/Ka I. The energy or net enthalpy of the adsorption process is represented by the constant b in the Langmuir equation. The free energy decreases with increasing values of the constant b , making the process more suitable since less energy is needed to maintain it. The process' endothermic nature is evident from the observed b value. For the adsorption of dyes on the adsorbents, the Freundlich equation was used. Table (4) provides K_f and n value information, Adsorption intensity (n) is a measure of the bond energies between the dye and the adsorbent. The fact that the values of n are greater than one suggests that the adsorption is suitable[27]. The results demonstrated that Ti/Ka I and Ti/Ka II both favorably adsorb the dye because their values of n are higher than unity.

Table.3. Freundlich and Langmuir constants and statistical parameters for Methylene blue dye

Adsorbent	Freundlich constants			Langmuir constants		
	K_f	n	R^2	Q_m	b	R^2
Ti/Z I	5.95	1.66	0.91	12.5	0.95	0.92
Ti/Z II	54.59	0.87	0.93	66.66	1.87	0.97

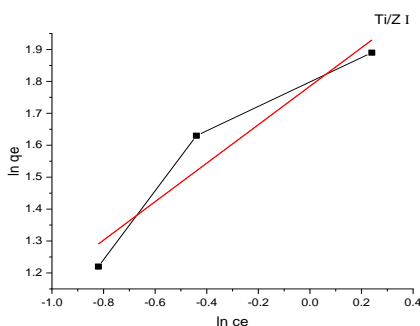


Fig. 15a. linear Freundlich isotherm for the adsorption of methylene blue dye by Ti/Z I

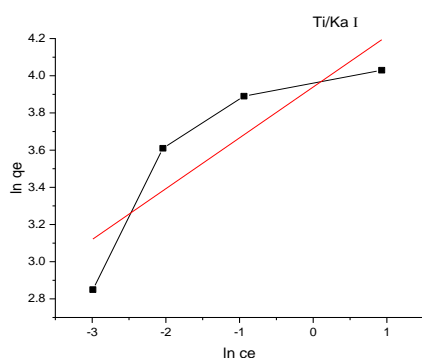


Fig. 15b. linear Freundlich isotherm for the adsorption of methylene blue dye by Ti/Ka I

Table 4. Freundlich and Langmuir constants and statistical parameters for Methylene blue dye

Adsorbent	Freundlich constants			Langmuir constants		
	K_f	n	R^2	Q_m	b	R^2 [5]
Ti/Ka I	2.97	1.47	0.99	4.34	11.52	0.99
Ti/Ka II	50.90	3.70	0.76	58.82	17.0	0.99

8. Conclusion

One of the major problems nowadays is the purification of waste water from textile fabrics. This study deals with removal of MB by two solids prepared by different methods from cheap origin as zeolite and kaolin doped by TiO_2 . Four prepared solids Ti/Z I, Ti/Z II, Ti/Ka I and Ti/Ka II were prepared by impregnation with calculated 10 and 15 m.mole of titanium oxide solid over zeolite and kaolin as supported materials. Textural characteristics for the prepared solids were examined by EDX, TGA&DTA, XRD, SEM, TEM and BET. It was found that the prepared solids had nano particles. These solids were used for removal of MB dye from aqueous solution at different Kinetic conditions as (effect of weight of adsorbents, concentration of MB dye, contact time and pH). It was found that the Ti/Ka II had maximum removal 99.9% at concentration of dye 10 ppm, weight of adsorbents 0.01g, contact time 120 min and pH = 3.

9. Conflicts of interest

There is no any conflict of interest

10. Formatting of funding sources

Self – funding

11. Acknowledgments

All facilities provided by Faculty of Women for Arts, Science and Education, Ain Shams University are greatly appreciated.

12. References

- [1] Belachew, N. and H. Hinsene, Preparation of zeolite 4A for adsorptive removal of methylene blue: optimization, kinetics, isotherm, and mechanism study. *Silicon*, 2022. 14(4): p. 1629-1641.
- [2] Jodeh, S., et al., Removal of methylene blue from industrial wastewater in Palestine using polysiloxane surface modified with bipyrazolic tripodal receptor. *Moroccan Journal of Chemistry*, 2016. 4(1): p. 4-1 (2016) 140-156.
- [3] Said, A., M.S. Hakim, and Y. Rohyami. The effect of contact time and pH on methylene blue removal by volcanic ash. in *Int'l Conference on Chemical, Biological, and Environmental Sciences*. 2014.
- [4] EL-Mekkawi, D.M., F.A. Ibrahim, and M.M. Selim, *Removal of methylene blue from water using zeolites prepared from Egyptian kaolins collected from different sources*. *Journal of Environmental Chemical Engineering*, 2016. 4(2): p. 1417-1422.
- [5] Rida, K., S. Bouraoui, and S. Hadnine, *Adsorption of methylene blue from aqueous solution by kaolin and zeolite*. *Applied Clay Science*, 2013. 83: p. 99-105.
- [6] Dyer, A., et al., *The use of zeolites as slow release anthelmintic carriers*. *Journal of helminthology*, 2000. 74(2): p. 137-141.
- [7] Król, M., *Natural vs. synthetic Zeolites*, 2020, Multidisciplinary Digital Publishing Institute.
- [8] Khaleque, A., et al., Zeolite synthesis from low-cost materials and environmental applications: A review. *Environmental Advances*, 2020. 2: p. 100019.
- [9] Saraya, M.E. and M.S. Thabet, *Characterization and evaluation of natural zeolite as a pozzolanic material*. *Al-Azhar Bulletin of Science*, 2018. 29(1-A): p. 17-34.
- [10] Derbe, T., S. Temesgen, and M. Bitew, *A Short Review on Synthesis, Characterization, and Applications of Zeolites*. *Advances in Materials Science and Engineering*, 2021. 2021.
- [11] Collins, F., et al., A critical review of waste resources, synthesis, and applications for Zeolite LTA. *Microporous and mesoporous Materials*, 2020. 291: p. 109667.

- [12] Snellings, R., G. Mertens, and J. Elsen, *Supplementary cementitious materials*. Reviews in Mineralogy and Geochemistry, 2012. 74(1): p. 211-278.
- [13] Khamchin Moghaddam, F., R. Sri Ravindrarajah, and V. Sirivivatnanon. Properties of Metakaolin Concrete—A Review. in International Conference on Sustainable Structural Concrete. 2015.
- [14] Siddique, R., *Waste materials and by-products in concrete*. 2007: Springer Science & Business Media.
- [15] Khatib, J.M., O. Baalbaki, and A.A. ElKordi, *Metakaolin, in Waste and Supplementary Cementitious Materials in Concrete*. 2018, Elsevier. p. 493-511.
- [16] Narmatha, M. and T. Felixkala, *Meta kaolin—the best material for replacement of cement in concrete*. IOSR Journal of Mechanical and Civil Engineering, 2016. 13(4): p. 66-71.
- [17] De Belie, N., M. Soutsos, and E. Gruyaert, Properties of fresh and hardened concrete containing supplementary cementitious materials. Vol. 25. 2018: Springer.
- [18] Lin, R.-S., Y. Han, and X.-Y. Wang, Experimental study on optimum proportioning of Portland cements, limestone, metakaolin, and fly ash for obtaining quaternary cementitious composites. Case Studies in Construction Materials, 2021. 15: p. e00691.
- [19] Sullivan, M.S., et al., Sustainable materials for transportation infrastructures: Comparison of three commercially-available metakaolin products in binary cementitious systems. Infrastructures, 2018. 3(3): p. 17.
- [20] Haider, A.J., Z.N. Jameel, and I.H. Al-Hussaini, *Review on: titanium dioxide applications*. Energy Procedia, 2019. 157: p. 17-29.
- [21] Bagheri, S., N. Muhd Julkapli, and S. Bee Abd Hamid, *Titanium dioxide as a catalyst support in heterogeneous catalysis*. The scientific world journal, 2014. 2014.
- [22] Dwivedi, G., G. Munjal, and A.N. Bhaskarwar, *Natural dye-sensitized solar cells with polyaniline counter electrode*. International Proceedings of Chemical, Biological and Environmental Engineering, 2015. 90.
- [23] Fatkhasari, Y., et al., Synthesis of TiO₂/Zeolite-A Composite for The Removal of Methylene Blue on Direct Sunlight. Jurnal Teknik ITS, 2019. 8(2): p. F115-F120.
- [24] Aziztyana, A.P., et al. Optimisation of methyl orange photodegradation using TiO₂-zeolite photocatalyst and H₂O₂ in acid condition. in IOP Conference Series: Materials Science and Engineering. 2019. IOP Publishing.
- [25] Olaremu, A., et al., *Synthesis of zeolite from kaolin clay from Erusu Akoko southwestern*. Journal of Chemical Society of Nigeria, 2018. 43(3).
- [26] Mouni, L., et al., Removal of Methylene Blue from aqueous solutions by adsorption on Kaolin: Kinetic and equilibrium studies. Applied Clay Science, 2018. 153: p. 38-45.
- [27] Jamil, T.S., et al., Removal of methylene blue by two zeolites prepared from naturally occurring Egyptian kaolin as cost effective technique. Solid State Sciences, 2011. 13(10): p. 1844-1851.